PCCP

Accepted Manuscript

ROYAL SOCIETY OF CHEMISTRY

www.rsc.org/pccp

Journal Name

ARTICLE

Activation of CO_2 by ionic liquid EMIM-BF_4 in the electrochemical system, a theoretical study

Received 00th January 20xx,
Accepted 00th January 20xx

DOI: 10.1039/x0xx00000x

www.rsc.org/

Yuanqing Wang,[a] Makoto Hatakeyama,[a] Koji Ogata,[a] Masamitsu Wakabayashi,[a] Fangming Jin,[b] and Shinichiro Nakamura[a*]

The electrochemical reduction of CO_2 to CO by an ionic liquid EMIM-BF_4 is one of the most promising CO_2 reduction processes proposed so far with its high Faradaic efficiency and low overpotential. However, the details of reaction mechanism are still unknown due to the absence of fundamental understandings. In this study, the most probable and stable geometries of EMIM-BF_4 and CO_2 were calculated by quantum chemistry in combination with exhaustive searches. A possible reaction pathway from CO_2 to CO catalyzed by EMIM-BF_4, including the most plausible intermediates and the corresponding transition states, was proposed. The role of EMIM-BF_4 is explained as forming a complex of $[EMIM\text{-}COOH]^-$ with CO_2 followed by decomposing to CO.

1. Introduction

Nowadays, oil, natural gas and coal are used as our main energy sources all over the world. The concerns about the anticipated depletion of fossil fuels have intrigued the need of developing sustainable energy sources, such as solar energy, wind and biomass. At the same time, the combustion of these fossil fuels probably leads to the increase of CO_2 concentration in the atmosphere from a preindustrial level of about 280 ppm to more than 390 ppm and maybe higher in the future.[1] The CO_2, greenhouse gas, is thought to be a main cause of global warming. Although there is some uncertainty and debate on the relationship between CO_2 emission and global warming, the utilization of CO_2 as a C1 building block for fuels and chemicals by using sustainable energy is highly desirable for energy transformation. At present, plenty of methods and technologies for utilizing CO_2 have been proposed from biological to chemical approaches.[2-4] In the chemical approaches, photocatalytic, electrochemical and photoelectrochemical reduction of CO_2 are intensively investigated because they can directly or indirectly use the sustainable energy source of sunlight. Electrochemical reduction of CO_2 can proceed through two-, four-, six-, and eight-electrons to produce carbon monoxide or formic acid, carbon or formaldehyde, methanol and methane, respectively. As seen in Eq. 1, it is commonly accepted that formation of $CO_2^{\bullet -}$ anion radical is an initial step for the electrochemical reduction of CO_2, which needs a very negative potential to force the reaction occur.[5, 6]

$$CO_2 + e^- = CO_2^{\bullet -} \qquad E = -1.90 \text{ V } \textit{vs.} \text{ NHE} \quad (1)$$

The more positive standard electrode potentials of producing CO, HCOOH, HCHO, CH_3OH and CH_4 (listed in Table S1, see Supporting Information, SI)[6] indicate a high overpotential needed to overcome the initial step. On the other hand, from a kinetic point of view, the reduction of CO_2 is also not easy since CO_2 is a highly inert molecule, which has a high activation barrier to overcome.

In addition, it faces the following problems: poor selectivity or low Faradaic Efficiency (FE), rapid loss of activity and the competing hydrogen production. One strategy to solve these problems is to add some electrocatalysts, such as transition metals,[2] to lower the overpotential by forming some complex. Recently, Bocarlsy and coworkers proposed a promising way of reducing CO_2 to methanol in the presence of pyridine with low overpotential achieving nearly 100% FE,[7-11] in which the role of pyridine and detailed mechanism are still on debate.[10] The formation of complex between CO_2 and pyridine derivatives is considered as the key step for reduction of CO_2 by many researchers.[10-15] Rosen et al.[16] reported a highly efficient method of reduction of CO_2 selectively to CO at the overpotentials below 0.2 volts catalyzed by a ionic liquid called "EMIM-BF_4" as shown in Fig. 1(a). The FE of CO was larger than 96%.[16] Other benefits of this technology are that ionic liquid itself is an electrolyte and CO_2 is remarkably soluble in the

[a] Nakamura Laboratory, RIKEN Innovation Center, 2-1 Hirosawa, Wako, Saitama 351-0198, Japan. E-mail: snakamura@riken.jp.
[b] School of Environmental Science and Engineering, Shanghai Jiao Tong University, 800 Dongchuan Road, Shanghai 200240, China.

Electronic Supplementary Information (ESI) available: optimized structures of EMIM-BF_4; a schematic strategy of generating input structures of EMIM-BF_4 and CO_2; relaxed potential energy surface scan with rotating –COOH group of carboxylic acid; comparison of calculated and experimental ^{13}C NMR spectrum of carboxylate and carboxylic acid at different total charges; energy diagram of reaction of carbene and CO_2; molecular orbitals of **4** and **6;** standard electrode potentials of reduction of CO_2 in aqueous solutions; analysis of vibration frequencies of possible intermediates in the presence of BF_4^- anion; validation of calculation methods for pKa values; and coordinates of molecular structures. See DOI: 10.1039/x0xx00000x.

imidazolium-based ionic liquids. In fact, the solubility of CO_2 in

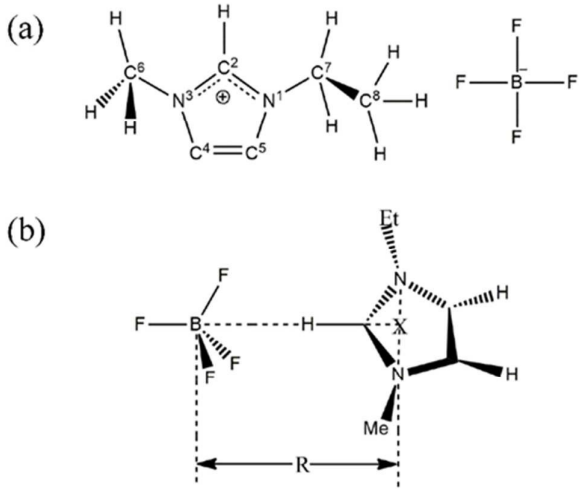

Fig. 1 Chemical structure of EMIM-BF_4. R is the distance between boron atom and the point X. The point X is the midpoint of two nitrogen atoms, which is close to the positive charge center of $EMIM^+$ cation.[18]

situ spectroscopy of Sum Frequency Generation (SFG) showed that the adsorbed EMIM layer on electrode surface can react with CO_2 to form a complex such as CO_2-EMIM which was then converted to CO as shown in Fig. 2(a).[19] The reaction rate depends remarkably on the metal electrode employed. The addition of water to EMIM-BF_4 dramatically increases the efficiency of CO_2 conversion to CO. It is possibly due to the increased proton by the hydrolysis of tetrafluoroborate.[20] A recent research employing Bi-based electrode confirms that ionic liquid has a significant effect of increase in the electrochemical reduction of CO_2 to CO.[21, 22] Furthermore, anions of ionic liquid have influence on the FE of reduction of CO_2 to CO in the order: $OTf^- > PF_6^- = BF_4^- > Cl^- > Br^-$.[22]

As shown in Fig. 2(c), a carboxylate species was found as an intermediate in acetonitrile by ^1H NMR and ^{13}C NMR analysis of electrolysis samples by Sun et al.[23] The charge of species (negative or neutral) and whether it was protonated or not, have not been determined yet. More importantly, they considered that the production of carboxylate (Fig. 2 (c)) was just a side reaction competing with the actual CO production, based on the fact that another ionic liquid MMMIM-Tf_2N, which cannot produce carboxylate, showed better FE for CO.[23] Because there is no proton at C2 position of $MMMIM^+$ in this ionic liquid (MMMIM-Tf_2N), the deprotonation of cation to carbene is not expected, while the formation of carbene was assumed indispensable to the carboxylate products by the carboxylation of C2 in carbene with CO_2 (Fig. 2(d)).[23, 24] Moreover, they proposed a mechanism including adsorbed $CO_2^{\bullet-}$ stabilized by adsorbed cation of ionic liquid (Fig. 2(b)). However, where the other oxygen of CO_2 goes, as the CO is reduced, is not very clear in this proposed mechanism. A preliminary calculation was performed to examine the

increases; reaching 0.72 mole fraction CO_2 in BMIM-PF_6 at 93 bar.[17] An *in-*

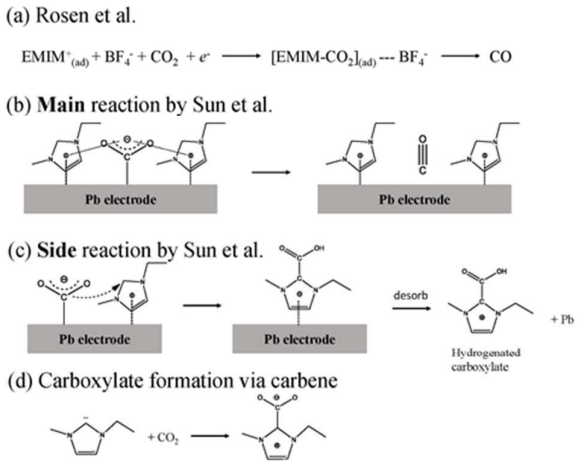

proposed main reaction mechanism assuming that the oxygen atom bonds to one Pb layer atom after the reaction as shown in Eq. 2 and Fig. S1, ESI. It was found that the reaction energy

Fig. 2 Proposed reaction mechanism for CO production with ionic liquid by (a) Rosen et al.[19] and (b), (c) Sun et al.[23] and (d) carboxylate formation via carbene[24].

$$Pb(111) + 2EMIM^+ + CO_2^{\bullet-} = Pb(111)\text{-}O^- + 2EMIM^+ + CO \quad (2)$$

change is 26.6 kcal/mol, suggesting it is thermodynamically unfavourable. As a matter of fact, the absence of proton at C2 position of $MMMIM^+$ cannot always exclude the possibility of the carboxylate formation, even though $MMMIM^+$ cannot form carbene. In other words, the reaction mechanism of CO_2 and MMMIM-Tf_2N may also contain a carboxylate intermediate, not necessarily from the carbene pathway, to be discussed in section 3.3.3. It should be addressed that the debates on the effect of proton concentration show the complexity of the reaction mechanism. More than one mechanism may exist according to the structure of ionic liquid and type of solvent (aqueous or non-aqueous). In the case of EMIM-BF_4 and water, Rosen et al.[20] suggested that a higher proton concentration could lower the barrier and enhance the rate, while in the case of EMIM-Tf_2N and acetonitrile, Sun et al.[23] found no change of the CO amount by adjusting proton concentration. Zhou et al.[25] found that high proton concentration (pH=1.7) in water would favour hydrogen production but not CO.

The details of the reaction pathways and their mechanism of the electrochemical CO_2 reduction in ionic liquid are still unknown. The questions to be answered are:

(i) What is the exact geometry and electronic structure of the intermediates? How do they stabilize the high energy $CO_2^{\bullet-}$ anion radical? Namely, how does ionic liquid catalyze the reaction? (ii) Are electron transfer (ET) and proton transfer (PT) to CO_2 stepwise or concerted? If they are stepwise, does proton transfer precede electron transfer or vice versa? (iii)

Why does this reaction system have an excellent selectivity for CO?

In an attempt to answer these questions, we applied density functional theory calculation for:

(i) identifying the possible intermediates and evaluating electrode potential, pKa and vibrational frequencies comparing with experimental results, and (ii) determining the thermodynamically and kinetically viable reaction pathways, through the identification of intermediates and transition states.

The answers to these questions provide a guiding principle to future catalyst design for electrochemical CO_2 reduction. In the present study, we focus on the electrochemical reduction of CO_2 by EMIM-BF_4 in aqueous solution by density functional theory (DFT) methods. Very recently, it was shown that DFT methods should be taken very carefully in several cases, especially in proton-shuttle pathway, since it may lead to consistently large energetic error.[26]

2. Calculation methods

The calculations are performed using DFT-B3LYP and MP2 methods combined with either aug-cc-pVDZ, 6-31++G(d,p), or 6-31G(d,p) basis set as implemented in Gaussian 09 packages.[27] A mixed restricted/unrestricted calculation method was used, and the free energies obtained by both methods have no significant difference. The conductor-like polarizable continuum implicit solvent model (CPCM)[28, 29] with set of UAHF radii was employed to describe the effects of solvation unless otherwise stated. The D3 version of Grimme's dispersion with Becke-Johnson damping[30] was added in some cases to include dispersion energy. Acidity constants (pKa) of species AH^+ (Eq. 3) were evaluated by calculating aqueous phase deprotonation free energies difference, given from Eq. 4,[12]

$$A+H^+ \leftrightarrow AH^+ \quad (3)$$

$$pK_a=-\log K_a=\frac{G_{298}(A)+G_{298}(proton)-G_{298}(AH^+)}{2.303\cdot RT} \quad (4)$$

where R is the gas constant, T is the absolute temperature which is set at 298 K in this study and G_{298} is absolute free energies at 298 K. An empirical value is generally used for the free energy of a proton in solution: -270.3 kcal/mol.[12]

Redox potential of Eq. 5 was calculated from Eq. 6,[31]

$$A+n_e e^-+n_H H^+ \rightarrow AH_{n_H}^{(n_H-n_e)} \quad (5)$$

$$E_{1/2}=-\left(\frac{\Delta G_{1/2}^0}{n_e F}\right)-\frac{R\times T\times \ln(10)\times n_H}{n_e F}\,pH-E_{1/2}^{0,ref} \quad (6)$$

where F is Faraday's constant, n_e and n_H is the number of electrons and protons, respectively. $E_{1/2}{}^{0,ref}$ is the reference potential (usually either standard hydrogen electrode (SHE) at 4.281 V[12] or the standard calomel electrode (SCE) at 0.24 V relative to SHE), and $\Delta G_{1/2}{}^0$ is determined from Eq. 7.

$$\Delta G_{1/2}^0=G_{298}\left(AH_{n_H}^{(n_H-n_e)}\right)-G_{298}(A)-n_H G_{298}(H^+) \quad (7)$$

Energy contributions due to an applied electrode potential, φ (*vs.* SHE or SCE), were modeled by adding $-n_eF(-\varphi-E_{1/2}{}^{0,ref})$ to $\Delta G_{1/2}{}^0$ following each electrochemical reduction step (Eq. 8),[32, 33]

$$\Delta G^0=\Delta G_{1/2}^0-n_e G\left(e^-\right)=\Delta G_{1/2}^0-n_e F(-\emptyset-E_{1/2}^{0,ref}) \quad (8)$$

where ΔG^0 is the standard reaction free energies and $G(e^-)$ is the energy of free electron.

3. Results and discussion

3.1 Geometry of EMIM-BF_4 and CO_2

3.1.1 Geometry of two-body system: EMIM-BF_4. Structures of $EMIM^+$ and BF_4^- are shown in Fig. 3. As the initial guess geometries we put one BF_4^- anion around the $EMIM^+$ cation at eight representative positions. They are above and below the plane of $EMIM^+$ cation and near C6, C7, N4 or N5 atoms, respectively. Four types of stable structures of EMIM-BF_4 in the gas phase were obtained, as shown in Fig. 3 (for details see Fig. S2, ESI). Their geometry parameters are shown in Table 1. Top_1 and top_2 show more stable structure than side_1 and side_2. The energy difference is relatively small between side_1 and side_2, or top_1 and top_2. It is just due to the rotation of ethyl group or BF_4^- anion. In order to include the neglected dispersion energy caused by B3LYP, empirical dispersion energies were added and high level method (MP2) was also used. The neglected dispersion energies were estimated at about 23 kcal/mol by single point calculations for these four structures. As shown in Table 1, the biggest relative energy difference is within 1.3 kcal/mol, showing that the gross energy difference is not affected by dispersion energy correction.[34] The results using MP2 method showed the similar behaviour that top conformers are more stable than side conformers for about 10 kcal/mol.

An estimation of the ionic strength of interaction can be obtained from ion-pair dissociation energy as defined[35] below (Eq. 9).

$$\text{Dissociation Energy}=E_{cation}+E_{anion}-E_{ion\text{-}pair} \quad (9)$$

The calculated dissociation energy are around 86 kcal/mol for side conformers and 96-98 kcal/mol for top conformers which are comparable with the results of BMIM-BF_4 (about 82 kcal/mol) reported by Hunt et al.[35] The interaction between $EMIM^+$ cation and BF_4^- anion mainly consists of the electrostatic energy,[36] hydrogen bond[37] and dispersion[34] that determine the stable structure of complexes. The isotropic charge-charge interaction is reported to be the main term of the electrostatic energy in ionic liquids.[36] Thus, the interaction between the

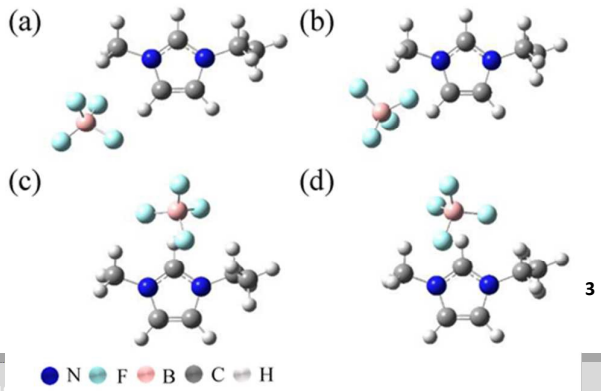

Fig. 3 Optimized structures of EMIM-BF_4. (a) side_1; (b) side_2; (c) top_1; (d) top_2. "side" represents the position of BF_4^- anion is located aside the $EMIM^+$ cation and the position of boron is approximately in the cation plane. "top" represents the position of BF_4^- anion is located above the $EMIM^+$ cation plane. Calculation method of B3LYP/6-31G(d,p) is used.

Table 1 Geometry parameters of optimized EMIM-BF_4

State	Energy/ B3LYP (kcal/mol)	Energy/ MP2 (kcal/mol)	Mulliken Charges of $EMIM^+$	Mulliken Charges transfer	R(Å)	Distance from H in C2 to F (Å)	Angle of C2-H---F	Dissociation Energy/B3LYP (kcal/mol)
side_1	0.0 (0.0)	0.0	0.803	0.197	4.65	1.837	169.5	86.7
side_2	0.5 (0.2)	-	0.826	0.174	4.54	1.879	146.1	86.2
top_1	-10.9 (-12.2)	-11.2	0.775	0.225	3.70	1.945	138.1	97.6
top_2	-9.1 (-10.1)	-10.2	0.790	0.210	3.64	1.919	140.4	95.9

Method: B3LYP/6-31G(d,p) unless otherwise stated (MP2/6-31G(d,p)). The values in parentheses are obtained after dispersion energy correction. The meanings of notation, such as "side_1", were explained in Fig. 3.

anion and cation is determined by the distance R (Fig. 1 (b)) between anoin and imidazolium ring in some extent.[18] The low energies of top_1 and top_2 are probably due to their shorter distance between ions (Table 1). As shown in Table 1, there are close contacts between H atom in the imidazolium ring and F atom of BF_4^-, suggesting the existence of hydrogen bond. However, the angles of C2-H---F are not linear which are not similar with the conventional linear hydrogen bond. On the other hand, the exact definition of hydrogen bond in ionic liquids is in itself a difficult problem since the Coulombic interactions of the ions cannot be easily separated from the Coulombic component associated with hydrogen bond.[37] Note that top_1 structure is slightly more stable (about 1~2 kcal/mol) than top_2 structure, though the distance R of top_1 is a little bigger than that of top_2. It can be explained by the larger charge transfer from anion to cation in top_1 than that in top_2 (Table 1).

3.1.2 Geometry of three-body system: EMIM-BF_4 and CO_2. At the second step, we put the linear CO_2 molecule near the EMIM-BF_4 (two-body system) as the initial guess. As shown in Fig. S3, ESI, the plane of imidazolium ring was first put in the xy plane. We adopted four optimized geometries of EMIM-BF_4. We also adopted one crystal structure of EMIM-BF_4 found in Crystallography Open Database (COD ID: 4100974).[38]

As shown in Fig. S3, ESI, for each geometry of EMIM-BF_4, we put one CO_2 molecule along the x axis (a), y axis (b) or z axis (c) to surround EMIM-BF_4. The nearest distance between the atoms in EMIM-BF_4 and CO_2 was in the range from 1.5 Å to 2.0 Å. In total, 2487 input structures of (EMIM-BF_4 + CO_2) were examined. After the optimization, 1807 geometries out of 2487 were successfully converged. The rest non-converged guesses are most probably due to the chemically un-realistic positions. Amongst the 1807 optimized structures of (EMIM-BF_4 + CO_2) thus obtained, the most stable structure was selected as shown in Fig. 4(a). Comparing with the optimized structure in the absence of CO_2, the position of BF_4^- anion is still close to C2-H atom with similar distance of C2-H---F (1.874 Å) and R (3.81 Å). The CO_2 molecule is in the same side with BF_4^- anion to the imidazolium ring plane. The shape of O=C=O is a little bended (∠O-C-O: 175.4 degrees) due to the interaction between the CO_2 molecule and EMIM-BF_4. A theoretical calculation of (EMIM-OAc + CO_2)[39] also confirmed that this kind of configuration is the most stable one. The interactions between each pair (cation-anion, cation-CO_2 and anion-CO_2) are affecting each other and the strength varies in gas and neat ionic liquid.[39] Taking the energy of the most stable structure as reference

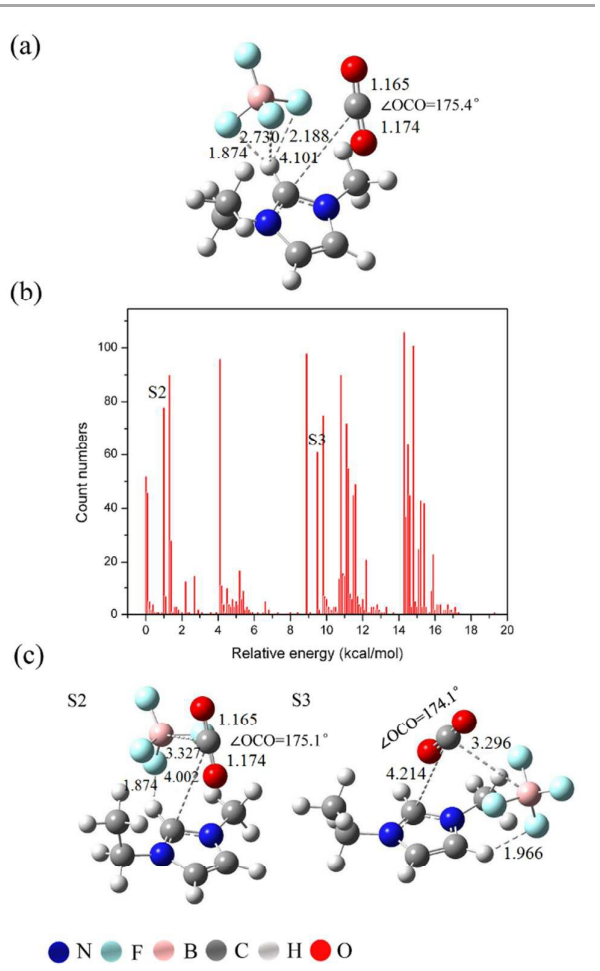

Fig. 4 (a) The lowest energy structure of EMIM-BF_4 and CO_2. R = 3.81 Å. (b) Histogram of full obtained structures according to energy. (c) Two selected structures. S2: relative energy = 1.1 kcal/mol (0.8 kcal/mol), R = 3.87 Å; S3: relative energy = 8.9 kcal/mol (9.1 kcal/mol), R= 4.34 Å. B3LYP/6-31G(d,p) is used. The values in parentheses are obtained after dispersion energy correction. The values in the figure are the distances between atoms in the unit of Å.

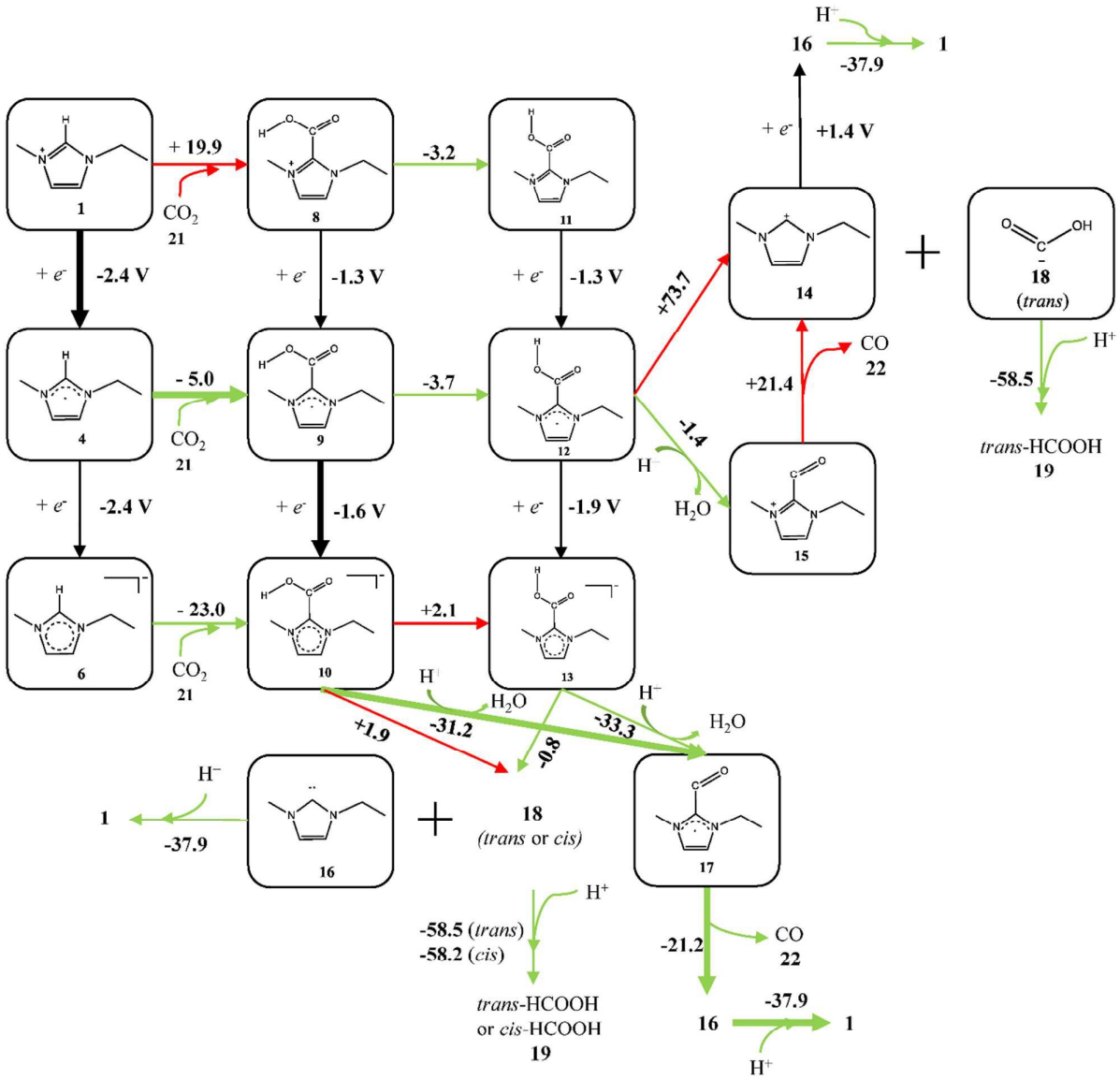

Fig. 5 A schematic flow of reaction intermediates. BF_4^- anion was not shown in the figure for simplicity. The values represent the calculated reaction free energies (kcal/mol) in each reaction step or standard electrode potential (V *vs.* SHE) in each electrochemical step. Green arrows represent the thermodynamically favorable pathway and red arrows represent unfavorable ones. The calculations were performed using B3LYP/6-31++G(d,p) level with implicit water (CPCM). Optimized structures of intermediate **18** (*trans* and *cis*) were obtained without the inclusion of UAHF set, otherwise they do not converge.

0.0 kcal/mol, the relative energies of other converged structures have been statistically shown by a histogram (Fig. 4(b)); the energies of other converged structures are approximately in the range 0 – 18 kcal/mol. Two representative structures were selected and shown in Fig. 4(c). The main difference was found in the position of BF_4^- anion, which may cause the total energy to increase. Significantly, the fact that the CO_2 molecule takes a position above the imidazolium ring indicates that the reactive site for CO_2 reduction may be the carbon or nitrogen atoms in the imidazolium ring.

3.2 Possible intermediates

As shown in Fig. 5, starting from the most stable structure of (EMIM-BF_4 + CO_2, Fig. 4(a)), the possible intermediates were generated. We took account of the following four aspects: (i) This reaction is a proton dependent process, since experimental results showed that protons effectively increase the FE of CO production.[20] Even in the absence of water, the FE for CO production was nearly 20%.[20] Experimental results[40] and theoretical research[41] both confirm that the hydrogen at C2 (C2-H) is more acidic than those at C4 or C5 in the imidazolium based ionic liquids, which can be a proton source in the absence of water. These results indicated that C2 or C2-H is a reactive site in

imidazolium based ionic liquid. (ii) In the reaction of **1** → **8** (see Fig. 5), for example, the carbon of the CO_2 attacks the carbon in the imidazolium ring accompanied by the C2-H bond fission and then proton transfers to oxygen of CO_2 resulting in the formation of –COOH. The formation of such imidazolium-2-carboxylate was monitored by Raman spectroscopy and DFT calculations.[42] The ^{1}H NMR and ^{13}C NMR results of electrolysis products of CO_2 and EMIM-Tf_2N in acetonitrile also support the formation of carboxylate during the electrochemical reaction.[23] After forming –COOH from carboxylate, there is an isomerization of C–OH rotation between **8** and **11**, **9** and **12**, **10** and **13**. The relaxation on the potential energy surface with rotating –COOH group of **8**, **9** and **10** (see Fig. S4, ESI) shows that multiple local minimum may exist at different dihedral angles which are between the imdazolium ring plane and –COOH group. The dihedral strains are estimated around 5 kcal/mol, 16 kcal/mol and 24 kcal/mol for **8**, **9** and **10**, respectively, showing the possibility of transformation between different configurations, especially for **8** and **9**. (iii) Proton-coupled electron transfer (PCET) reactions are widely accepted as the mechanistic pathways in electrochemistry.[43] It states that the electrochemical reactions proceeds through one proton and one electron transfer, step by step or in a concerted way.[43] In the former case, it is referred as sequential proton-electron transfer (SPET).[43] The latter case is referred as concerted proton-electron transfer (CPET).[43] For SPET, there will be two possibilities which are proton transfer (such as **1** → **8**) followed by electron transfer (such as **8** → **9**) and vice versa (such as **1** → **4** and **4** → **9**). For CPET, there will be a possibility such as diagonal reaction **1** → **9**, to be discussed later. The formation of one electron reduced imidazolium cation (like intermediate **4**) has been reported by experiments[44] and quantum calculations[45]. (iv) After the formation of intermediate **10**, **12** or **13**, CO or HCOOH can be selectively produced depending on the bond fission,[46] as shown in Scheme 1 and Fig. 5. One type of bond fission in C-O (type A) leads to CO, while the other in C-C fission (type B) leads to HCOOH (Scheme 1). From the intermediate **10**, *cis*-HCOOH may be formed, while *trans*-HCOOH may be formed from intermediates **12** and **13** after dissociation. Direct dissociation of intermediate **11** seems to be unreasonable without electron acceptance. It is not in agreement with the experimental results that the whole reactions take place in the electrochemical system.[16, 19] Besides, the NMR results from simple mixture of EMIM-Tf_2N and CO_2[23] do not support the carboxylate formation, indicating that **8** and **11** are not present in the reaction.

As shown in Fig. 5, taking account of these aspects, we have generated all the possible intermediates. The next task is to select these intermediates and to identify a favourable pathway, based on spectroscopic data and theoretical calculations. As mentioned above, carboxylate or carboxylic acid formation was proposed from NMR spectroscopy of electrolysis products of CO_2 and EMIM-Tf_2N.[23] However, neither the exact charge of the detected complex nor the exact structure (carboxylate or carboxylic acid) can be determined by NMR. Therefore, in this study, we formulated the possible charges, then calculated the relative chemical shift of carboxylate and carboxylic acid. As shown in Fig. S5, ESI, the calculated chemical shifts of all structures agree well with the experimental ones. To the best of our knowledge, it is the first time to confirm the presence of carboxylate or carboxylic acid

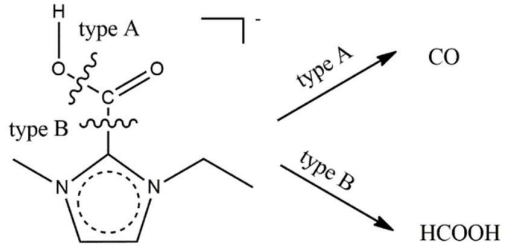

13

during the electrolysis of CO_2 in ionic liquids, from theoretical calculations.

Scheme 1 Plausible bond fission of intermediate **13** toward formation of CO or HCOOH

Especially, a resonance of 155.1 ppm in the ^{13}C NMR spectrum was observed and assigned to the carboxylate (or carboxylic acid) binding to C2 of the imidazolium ring.[23] The nearest result to this experimental value was obtained from a carboxylic acid with -1 charge (156.8 ppm) in this study (see red circles in Fig. S5, ESI). The formation of carboxylic acid is strongly suggested.

A vibrational frequency of 2348 cm^{-1} assigned to O=C=O stretching mode in EMIM-CO_2---BF_4 complex, which is considered as a key intermediate, has been reported by SFG.[19] As the potential extended from -0.2 V to -0.8 V, the size of the peak grew linearly. It indicates that the intermediate has received one or two electrons.[19] Therefore, we formulated the possible complexes of EMIM-BF_4 and CO_2 (intermediates **2**, **5** and **7**, similar configurations as shown in Fig. 4(a)), whose total charge are 0, -1 and -2, respectively (see Table S2, SI for detail structures). The vibrations of these carboxylic acids have been also examined to make a full investigation. As shown in Table S2, comparing the calculated frequencies of possible intermediates with the experimental value, we remark that the frequency of intermediate **5** is close to the experimental data. Thus, we conclude that the intermediate **5** is the species detected by SFG, namely, the complex of one electron received EMIM-BF_4 and CO_2. We rule out **2**, **8** and **11** from possible intermediates because they have no electrons received (see Fig. 5), i.e. not the species detected by SFG, although they have more close frequencies to experimental value.

3.3 Proposed mechanism

3.3.1 Reaction pathway. As shown in Fig. 5, there are many reaction pathways from EMIM-BF_4 and CO_2 to the final product CO. The calculated reaction free energies of each step suggest thermodynamically favourable paths as shown with green arrows. Unfavourable ones are shown with red arrows. The reactions caused by electron transfer from electrode are shown with black arrows. They can be thermodynamically favourable if appropriate bias is applied. The data presented in Fig. 5 show that the favourable reaction pathway (connected by green and black arrows) can be:

Path 1: **1** → **4** → **9** → **12** → **13** …→ CO or HCOOH

Alternative pathways (Path 2 and Path 3) are possible via intermediate **10**. The **10** does not necessarily undergo isomerization to intermediate **13**, since it is thermodynamically unfavourable. Thus, the direct way is from **10** to **17**.

Path 2: **1** → **4** → **9** → **10** → **17**…→ CO

Path 3: **1** → **4** → **6** → **10** → **17**…→ CO

As can be found in Fig. 5, once intermediate **10** or **13** is formed, the pathway to CO is thermodynamically more favoured than that to HCOOH, which is in accordance with the experimental results. Note that in the calculation of free energies in this section, the anion BF_4^- was not included in the model to simplify the system unless otherwise stated. The simplification can be justified by the thermodynamic and NMR spectroscopic studies for some imidazolium based ionic liquids.[47] It was reported that the ionic liquids were dissolved into constituent ions up to certain concentrations, which means both the cations and anions are solvated in a certain amount by water molecules.[47]

Fig. 6 presents an energy profile of three pathways at different applied potentials. At the applied bias of -2.4 V *vs.* SHE, all the steps in the reaction mechanism are zero or negative in reaction free energies. That is, -2.4 V should be the onset potential which is defined as the smallest applied potential needed to make all steps exergonic (downhill in free energy).[48] It shows that the step from intermediate **1** to **4** and **4** to **6** determines the value of onset potential. By contrast, at the applied bias of -0.25 V *vs.* SHE, the overall reactions are thermodynamically unfavourable (uphill in free energy). Experimental data, however, showed that the onset potential of reduction of CO_2 by EMIM-BF_4 is about -0.25 V *vs.* SHE.[19] The discrepancy between -2.4 V vs -0.25 V may be that the calculations were performed assuming a homogeneous system in which surface effects were not considered. The key step of electron transfer is in fact considered at the heterogeneous system.[15, 19] This homogeneous approximation may be the reason for the calculated over estimation of onset potential. Similar result has been reported in the calculation of reduction potential of PyH^+.[15] The reason why less negative potential needed on electrode surfaces is due to the neglect of adsorption and/or desorption process on the surface.

Comparing the three pathways, at the applied bias of -0.25 V, all the pathways are thermodynamically unfavourable, especially for Path 3. When the applied bias moves to more negative value (-2.4 V), Path 2 turns out to be more preferable reaction pathway than the others from a thermodynamic point of view, though the difference from Path 1 and 3 seems minor.

3.3.2 Carbene-mediated reaction mechanism. We have examined the possibility of the carbene-mediated mechanism for carboxylate formation from the origin of carbene in ionic liquid. Generally, there are two methods to generate carbene from ionic liquid. One is through the deprotonation induced by the strong base, such as acetate.[42, 49-51] Another is from the the electro-reduced imidazolium cation as shown in Eq. 10.[44, 52]

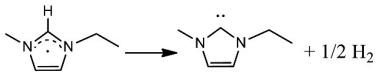

(10)

Firstly, we examined the deprotonation pathway. As shown in Fig.5, there are key steps in the hydrogenation of CO_2: steps **1** → **8**, **4** → **9** and **6** → **10**. Focusing on the reaction **1** → **8**, three elementary steps are to be considered due to the carbene reaction mechanism[23]: (i) deprotonation of EMIM-BF_4 at C2 position to form carbene; (ii) CO_2 reacts with carbene to produce carboxylate; (iii) reprotonation of carboxylate to form intermediate **8**. The pKa is to be considered since it was reported that BF_4^- anion seems to be

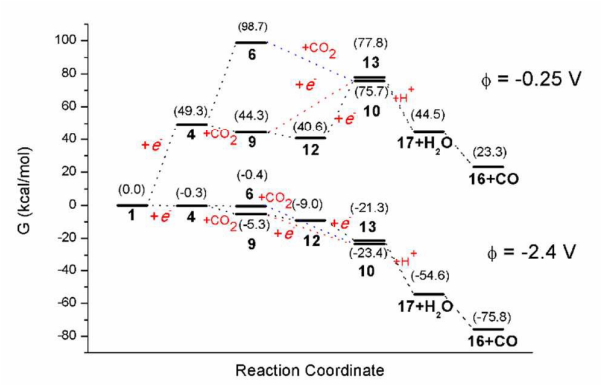

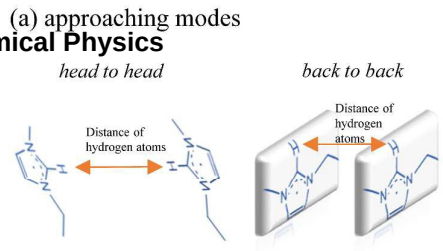

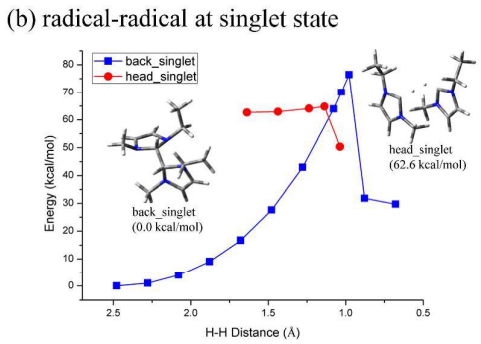

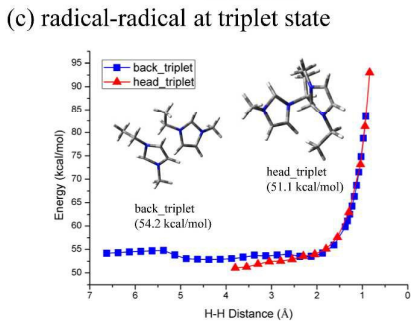

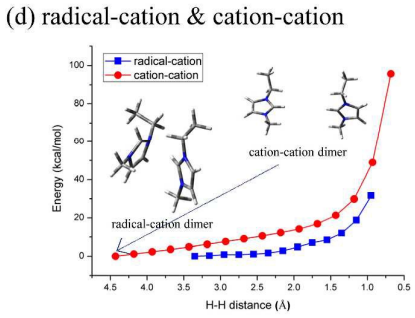

Fig. 6 A mechanistic summary depicting overall reaction free energies and their dependence on applied potentials. The values in parentheses are relative free energies in kcal/mol.

unable to deprotonate the imidazolium ring from the C2 position due to its small basicity.[49] Keith et al. proposed a methodology to calculate pKa which shows deprotonation ability of molecules.[12] In order to validate the method for pKa calculation in ionic liquids, we have chosen several typical ionic liquids. Then we compared the calculated results with their experimental values. Results are shown in Table S3 (see SI), where the calculated pKa values are fitted well with the experimental data. We conclude that the method is valid to evaluate pKa in ionic liquids. We then applied it to our own system. The calculated pKa values of EMIM-BF_4 and intermediates **4** and **6** (in the presence of anion) are 24.8, 48.4 and 68.2, respectively. They are too large, suggesting that they are unable to deprotonate even in the case after receiving electrons.[12] Although the existence of "abnormal" deprotonations at C4 and C5 positions of imidazolium cation in the presence of strong base acetate has been shown by experiments,[53] here we focus mainly on the reactions at C2 position. Because the pKa values at C4 and C5 positions for imidazolium cation are calculated to be 34.2 and 34.4, respectively, larger than that at C2 position. Besides, NMR results[23] and our calculations are in accordance with the carboxylate formation at C2 position, suggesting the deprotonations at C4 and C5 positions may not be dominant in the present system.

Then we examined the electro-generated pathway.[44, 52] The Gibbs free energy change of Eq. 10 was estimated to be -18.5 kcal/mol in aqueous solution in the B3LYP/6-31++G(d,p) level, confirming it is thermodynamically favourable. As shown in Fig. 7, assuming a dimer mechanism for Eq. 10, the potential energy curves as a function of H-H (H at C2 position) distance were plotted. In addition to radical-radical case, radical-cation and cation-cation cases were also considered. In the case of radical-radical (Fig. 7(b)), a very stable species with C2-C2 bond formation in singlet state (denoted as back_singlet) was suggested.[44] However, the subsequent H-H approaching makes energy increase largely (over 70 kcal/mol) which is unable to overcome. Another dimer in singlet state (head_singlet) in Fig 7(b) seems possible to produce carbene with reasonable activation barrier while its energy is much higher than that with C2-C2 bond formation indicating that it is unlikely to exist. In other cases (two radicals in triplet state, radical-cation and

Fig. 7 (a) two initial guesses for the dimer geometry. (b), (c) and (d) potential energy curve of dimer as a function of H-H distance. The structure shown here are optimized structures and used as a starting point for relaxed scan, except cation-cation case due to strong repulsion. The values in parentheses are relative energies. In (d), there is no need to distinguish between head to head and back to back initial guesses because they give similar curves. The calculations were performed at B3LYP/6-31G(d,p) level with dispersion correction.

cation-cation cases), the activation barriers for H-H bond formation all seem very high (over 29 kcal/mol), suggesting that they are kinetically unfavourable. On the other hand, in the presently studied system, the FE of hydrogen formation was always less than 3% in the experiments,[16] suggesting the effect of Eq. 10 is minor probably due to kinetic barrier. Furthermore, even it is formed, the protonation of carbene with proton from water due to its large pKa value will be a competitive step with CO_2. One surprising result from previous report[20] was that increasing water can enhance the CO_2 reduction, which is obviously not due to carbene-mediated mechanism. Therefore, at present, the possibility of carbene-mediated reaction mechanism in the steps of **1** → **8**, **4** → **9** and **6** → **10** can be less probable, but not fully ruled out.

As a natural extension, in the case of concentrated carbene formation, which is possible as mentioned above, we examined its reaction with CO_2, as shown in Fig. S6, ESI. The reaction of carbene with CO_2 to carboxylate is spontaneous and nearly instantaneous since the activation barrier is very small (2.4 kcal/mol). This result agrees well with the experimental studies of carbene's high reactivity toward CO_2.[24, 54, 55] In the case of negatively charged complex as shown in Fig. S6(b), ESI, the reaction is also thermodynamically and kinetically favourable. Once the

carboxylate is formed with low activation barrier, the protonation in polar solvent to form species such as 8 or 9 is possible. Therefore, the central problem for CO_2 reduction is the formation of carbene. It indicates that the optimal catalysts can be designed through tuning the anion basicity or electrochemical condition, which induces the carbene formation. This is an important future project.

3.3.3 Proton-coupled electron transfer: SPET or CPET? It is well accepted in the molecular electrochemistry studies[15, 32] that CO_2 reductions may follow SPET pathways; whereas in the surface electrochemistry studies,[48, 56, 57] CPET pathways would be assumed. As Koper[58] pointed out, however, there are many experimental examples of electrocatalytic reactions on metal surfaces that the decoupling of proton and electron transfer is very important. In this study, the steps from intermediate **4** → **9** and **6** → **10** are the proton-coupled electron transfer steps which, we believe, are the key steps in determining the activity of reaction. Thus, the two steps were investigated in detail by locating their intermediates and transition states with population analysis (Mulliken and CHelpG charges). As discussed earlier, the carbene-mediated reaction mechanism is unlikely in the present system. Alternative reaction mechanism is examined. As shown in Fig. S7, ESI, orbital analysis shows that HOMO of reactants (**4** and **6**) is localized on the C2 atom of ionic liquid, suggesting CO_2 attacks on the C2 atom electrophilically at first.

As shown in Fig. 8(a), intermediate **26** and **27** were proposed as the products of electrophilic attack with the C-C bond formation (bond length: 1.618 Å in **26** and 1.562 Å in **27**). No transition state is located in this downhill step by exhaustive search. The Mulliken/CHelpG charges of total CO_2 atoms in intermediates **26** and **27** are -0.58/-0.74 and -0.83/-0.84, respectively, indicating electron transfer to CO_2 molecule from charged ionic liquid which leads to the bending of CO_2 (∠O-C-O: 131.0 degrees in **26** and 127.0 degrees in **27**). The next step is the approaching of H from C2 toward O in the bended CO_2, with the extension of C2-H bond distance (Fig. 8(a)). Finally, the C2-H bond fission is followed by proton transfer to oxygen atom in CO_2. The H on C2 atom in these intermediates and transition states shows a positive charge, confirming it is a proton.

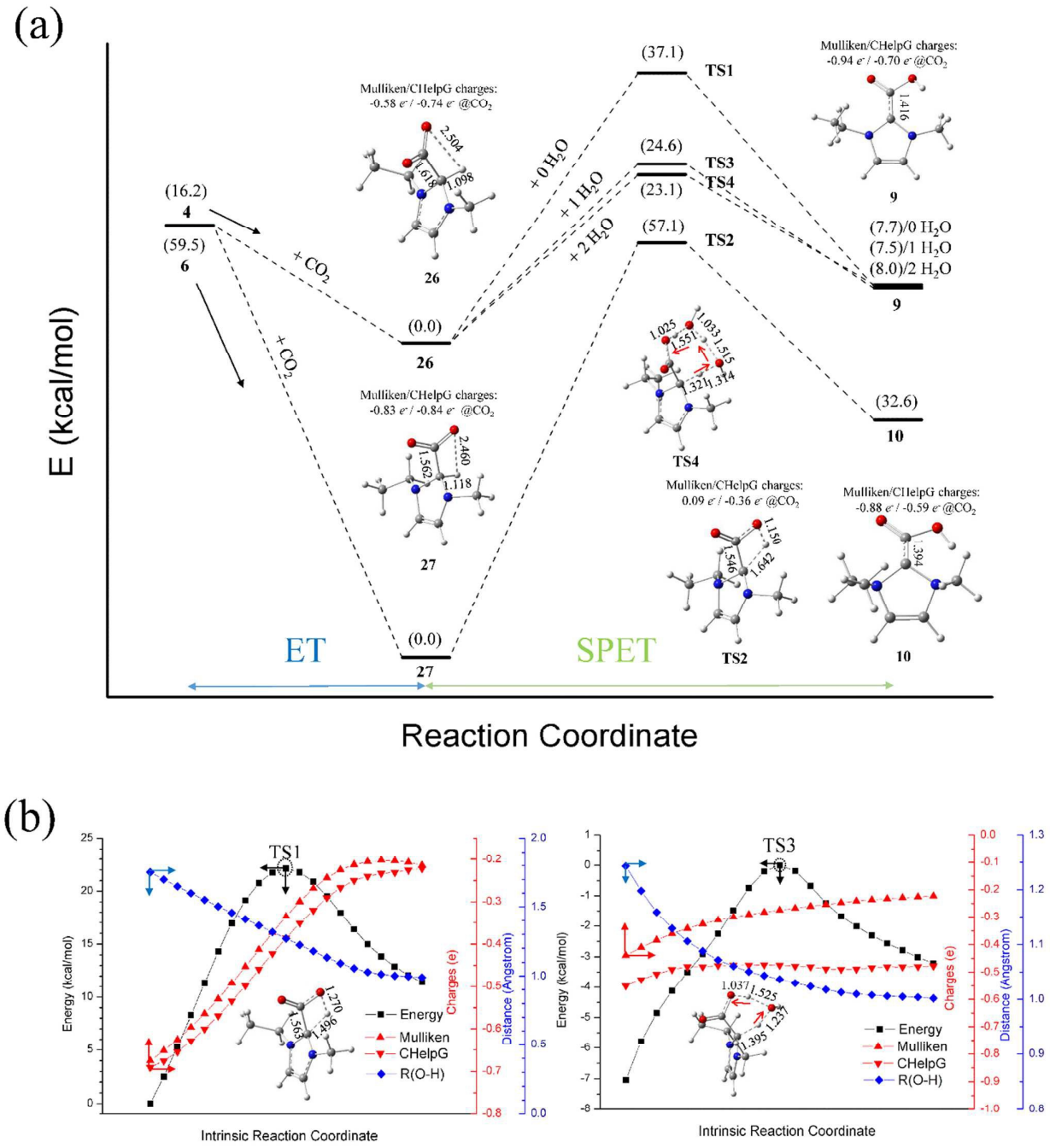

Fig. 8 (a) Electron transfer and proton transfer along the reaction from **4** to **9** and **6** to **10**. The values in parentheses are relative electronic energies in kcal/mol. Insects are molecular structures of intermediates and transition states. The values are distances between atoms (Å). The red arrows show proton transfer direction. (b) IRC calculations according to TS1 and TS3 structures. The Mulliken and CHelpG charges on CO_2 were calculated using the structures obtained along the intrinsic reaction coordinate. R(O-H) is the distance of O in CO_2 and H on C2. The calculations were performed at B3LYP/6-31++G(d,p) level with implicit water (CPCM). Radii option of UAHF in the solvation model was not specified in the calculation of this figure since transition structure cannot be found in the presence of UAHF set

As shown in Fig. 8(a), the activation barrier in the step of **26** → TS1 → **9** is smaller than that in **27** → TS2 → **10**. It indicates that **4** → **9** is favourable to **6** → **10** from a kinetic point of view. Remarkably, as shown in Fig. 8(a), owing to the interaction of water molecules through proton relay,[15] the activation barrier does decrease from 37.1 kcal/mol (TS1) to 24.6 kcal/mol (TS3, $1H_2O$) and further to 23.1 kcal/mol (TS4, $2H_2O$). It indicates that water can be a *co-catalyst* in this system to facilitate proton transfer, which is consistent with the experimental results, that is the enhancement role of water.[20, 25] Meanwhile, the variations of Mulliken/CHelpG charges in the species of the steps of **26** → TS1 → **9** and **27** → TS2 → **10** show that the electron density localized on CO_2 first decreases (less negative) and then increases along the proton transfer (Fig. 8(a)). Furthermore, population analysis (Fig. 8(b)) in the steps of **26** → TS1 → **9** and **26** + H_2O → TS3 → **9** + H_2O shows that the depletion of negative charges on CO_2 synchronizes with the O-H bond formation along the intrinsic reaction coordinate (IRC) as the distance of O (in CO_2) and H (on C2) decreases to ~ 1.0 Å. These results suggest that proton transfer and electron transfer to CO_2 are separated, that is, a SPET pathway (PT → ET) in this step. The electron transfer to CO_2 will be completed at **9** together with the rotation of –COOH group (not shown in Fig. 8(b)).

In summary, Path 2 is thermodynamically favourable to Path 1 and Path 3. Step **4** → **9** is favourable to **6** → **10** from a kinetic point of view, confirming the Path 2 containing the step of **4** → **9**. Fig. 9 presents the overall catalytic cycle from CO_2 to CO with EMIM-BF_4 as the electro-catalyst along with the pathways of Path 2.

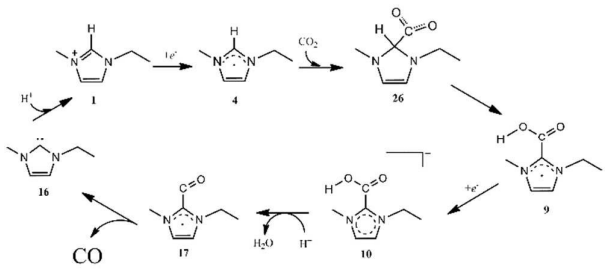

Fig. 9 Overall catalytic cycle mechanism (see Path 2).

4. Conclusions

The mechanism of a catalytic cycle to produce CO from CO_2 with EMIM-BF_4 as the electro-catalyst was proposed and compared with the experimental results. The calculations show that EMIM-BF_4 can effectively interact with CO_2 and form a key intermediate of $[EMIM\text{-}COOH]^-$ followed by decomposition to CO. The hydrogen in C2 position is considered to be the proton source to attach the CO_2 in forming the key intermediate. The subsequent proton-coupled electron transfer to CO_2 is shown to be a SPET (ET → PT → ET) pathway. Water itself can be a *co-catalyst* to facilitate proton transfer. The indirect proof of proposed intermediate EMIM-CO_2---BF_4 complex by SFG experiments was validated by the present DFT study. We believe that this theoretical study sheds light on the mechanism of CO_2 reduction catalysed by ionic liquids, and that provides the clue for the future catalyst design. The discrepancy between calculated and experimental onset potentials suggests the importance of electrode surface. The study including the electrode surface is ongoing.

Acknowledgements

We thank the RIKEN Integrated Cluster of Clusters (RICC) for supporting calculation resources.

Notes and references

1. NOAA. Website: http://www.esrl.noaa.gov/gmd/ccgg/trends.
2. J. L. Qiao, Y. Y. Liu, F. Hong and J. J. Zhang, *Chemical Society Reviews*, 2014, **43**, 631-675.
3. W. Wang, S. P. Wang, X. B. Ma and J. L. Gong, *Chemical Society Reviews*, 2011, **40**, 3703-3727.
4. J.-j. Hu, L. Wang, S.-p. Zhang, Y.-q. Wang and X.-f. Xi, *Bioresource Technology*, 2011, **102**, 7147-7153.
5. Y. Hori, in *Modern Aspects of Electrochemistry*, eds. C. Vayenas, R. White and M. Gamboa-Aldeco, Springer New York, 2008, vol. 42, ch. 3, pp. 89-189.
6. E. E. Benson, C. P. Kubiak, A. J. Sathrum and J. M. Smieja, *Chemical Society Reviews*, 2009, **38**, 89-99.
7. G. Seshadri, C. Lin and A. B. Bocarsly, *Journal of Electroanalytical Chemistry*, 1994, **372**, 145-150.
8. E. E. Barton, D. M. Rampulla and A. B. Bocarsly, *Journal of the American Chemical Society*, 2008, **130**, 6342-6344.
9. E. B. Cole, P. S. Lakkaraju, D. M. Rampulla, A. J. Morris, E. Abelev and A. B. Bocarsly, *Journal of the American Chemical Society*, 2010, **132**, 11539-11551.
10. Y. Yan, E. L. Zeitler, J. Gu, Y. Hu and A. B. Bocarsly, *Journal of the American Chemical Society*, 2013, **135**, 14020-14023.
11. Y. Yan, J. Gu and A. B. Bocarsly, *Aerosol and Air Quality Research*, 2014, **14**, 515-521.
12. J. A. Keith and E. A. Carter, *Journal of the American Chemical Society*, 2012, **134**, 7580-7583.
13. J. A. Keith and E. A. Carter, *Chemical Science*, 2013, **4**, 1490-1496.

14. M. Z. Ertem, S. J. Konezny, C. M. Araujo and V. S. Batista, *J Phys Chem Lett*, 2013, **4**, 745-748.
15. C. H. Lim, A. M. Holder and C. B. Musgrave, *Journal of the American Chemical Society*, 2013, **135**, 142-154.
16. B. A. Rosen, A. Salehi-Khojin, M. R. Thorson, W. Zhu, D. T. Whipple, P. J. A. Kenis and R. I. Masel, *Science*, 2011, **334**, 643-644.
17. L. A. Blanchard, Z. Gu and J. F. Brennecke, *The Journal of Physical Chemistry B*, 2001, **105**, 2437-2444.
18. S. Tsuzuki, H. Tokuda and M. Mikami, *Physical Chemistry Chemical Physics*, 2007, **9**, 4780-4784.
19. B. A. Rosen, J. L. Haan, P. Mukherjee, B. Braunschweig, W. Zhu, A. Salehi-Khojin, D. D. Dlott and R. I. Masel, *Journal of Physical Chemistry C*, 2012, **116**, 15307-15312.
20. B. A. Rosen, W. Zhu, G. Kaul, A. Salehi-Khojin and R. I. Masel, *Journal of the Electrochemical Society*, 2013, **160**, H138-H141.
21. J. L. DiMeglio and J. Rosenthal, *Journal of the American Chemical Society*, 2013, **135**, 8798-8801.
22. J. Medina-Ramos, J. L. DiMeglio and J. Rosenthal, *Journal of the American Chemical Society*, 2014, **136**, 8361-8367.
23. L. Sun, G. K. Ramesha, P. V. Kamat and J. F. Brennecke, *Langmuir*, 2014, **30**, 6302-6308.
24. H. A. Duong, T. N. Tekavec, A. M. Arif and J. Louie, *Chemical Communications*, 2004, DOI: 10.1039/B311350G, 112-113.
25. F. Zhou, S. Liu, B. Yang, P. Wang, A. S. Alshammari and Y. Deng, *Electrochemistry Communications*, 2014, **46**, 103-106.
26. R. E. Plata and D. A. Singleton, *Journal of the American Chemical Society*, 2015, **137**, 3811-3826.
27. M. J. Frisch, G. W. Trucks, H. B. Schlegel, G. E. Scuseria, M. A. Robb, J. R. Cheeseman, G. Scalmani, V. Barone, B. Mennucci, G. A. Petersson, H. Nakatsuji, M. Caricato, X. Li, H. P. Hratchian, A. F. Izmaylov, J. Bloino, G. Zheng, J. L. Sonnenberg, M. Hada, M. Ehara, K. Toyota, R. Fukuda, J. Hasegawa, M. Ishida, T. Nakajima, Y. Honda, O. Kitao, H. Nakai, T. Vreven, J. A. Montgomery Jr., J. E. Peralta, F. Ogliaro, M. J. Bearpark, J. Heyd, E. N. Brothers, K. N. Kudin, V. N. Staroverov, R. Kobayashi, J. Normand, K. Raghavachari, A. P. Rendell, J. C. Burant, S. S. Iyengar, J. Tomasi, M. Cossi, N. Rega, N. J. Millam, M. Klene, J. E. Knox, J. B. Cross, V. Bakken, C. Adamo, J. Jaramillo, R. Gomperts, R. E. Stratmann, O. Yazyev, A. J. Austin, R. Cammi, C. Pomelli, J. W. Ochterski, R. L. Martin, K. Morokuma, V. G. Zakrzewski, G. A. Voth, P. Salvador, J. J. Dannenberg, S. Dapprich, A. D. Daniels, Ö. Farkas, J. B. Foresman, J. V. Ortiz, J. Cioslowski and D. J. Fox, *Journal*, 2009.
28. M. Cossi, N. Rega, G. Scalmani and V. Barone, *Journal of Computational Chemistry*, 2003, **24**, 669-681.
29. V. Barone and M. Cossi, *The Journal of Physical Chemistry A*, 1998, **102**, 1995-2001.
30. S. Grimme, J. Antony, S. Ehrlich and H. Krieg, *The Journal of Chemical Physics*, 2010, **132**, 154104.
31. T. F. Hughes and R. A. Friesner, *The Journal of Physical Chemistry B*, 2011, **115**, 9280-9289.
32. J. A. Keith, K. A. Grice, C. P. Kubiak and E. A. Carter, *Journal of the American Chemical Society*, 2013, **135**, 15823-15829.
33. P. Liao, J. A. Keith and E. A. Carter, *Journal of the American Chemical Society*, 2012, **134**, 13296-13309.
34. P. A. Hunt and I. R. Gould, *The Journal of Physical Chemistry A*, 2006, **110**, 2269-2282.
35. P. A. Hunt, I. R. Gould and B. Kirchner, *Australian Journal of Chemistry*, 2007, **60**, 9-14.
36. S. Tsuzuki, H. Tokuda, K. Hayamizu and M. Watanabe, *The Journal of Physical Chemistry B*, 2005, **109**, 16474-16481.
37. I. Skarmoutsos, D. Dellis, R. P. Matthews, T. Welton and P. A. Hunt, *The Journal of Physical Chemistry B*, 2012, **116**, 4921-4933.
38. A. R. Choudhury, N. Winterton, A. Steiner, A. I. Cooper and K. A. Johnson, *Journal of the American Chemical Society*, 2005, **127**, 16792-16793.
39. O. Hollóczki, D. S. Firaha, J. Friedrich, M. Brehm, R. Cybik, M. Wild, A. Stark and B. Kirchner, *The Journal of Physical Chemistry B*, 2013, **117**, 5898-5907.
40. L. Crowhurst, P. R. Mawdsley, J. M. Perez-Arlandis, P. A. Salter and T. Welton, *Physical Chemistry Chemical Physics*, 2003, **5**, 2790-2794.
41. P. A. Hunt, B. Kirchner and T. Welton, *Chemistry – A European Journal*, 2006, **12**, 6762-6775.
42. M. I. Cabaço, M. Besnard, Y. Danten and J. A. P. Coutinho, *The Journal of Physical Chemistry A*, 2012, **116**, 1605-1620.
43. M. T. M. Koper, *Chemical Science*, 2013, **4**, 2710-2723.
44. L. Xiao and K. E. Johnson, *Journal of the Electrochemical Society*, 2003, **150**, E307-E311.
45. M. C. Kroon, W. Buijs, C. J. Peters and G.-J. Witkamp, *Green Chemistry*, 2006, **8**, 241-245.
46. I. M. B. Nielsen and K. Leung, *The Journal of Physical Chemistry A*, 2010, **114**, 10166-10173.
47. T. Singh and A. Kumar, *Vib Spectrosc*, 2011, **55**, 119-125.
48. A. A. Peterson, F. Abild-Pedersen, F. Studt, J. Rossmeisl and J. K. Norskov, *Energy & Environ Sci*, 2010, **3**, 1311-1315.
49. O. Holloczki, D. Gerhard, K. Massone, L. Szarvas, B. Nemeth, T. Veszpremi and L. Nyulaszi, *New Journal of Chemistry*, 2010, **34**, 3004-3009.
50. G. Gurau, H. Rodríguez, S. P. Kelley, P. Janiczek, R. S. Kalb and R. D. Rogers, *Angewandte Chemie International Edition*, 2011, **50**, 12024-12026.
51. O. Hollóczki and L. Nyulászi, in *Electronic Effects in Organic Chemistry*, ed. B. Kirchner, Springer Berlin Heidelberg, 2014, vol. 351, ch. 416, pp. 1-24.
52. B. Gorodetsky, T. Ramnial, N. R. Branda and J. A. C. Clyburne, *Chemical Communications*, 2004, DOI: 10.1039/B407386J, 1972-1973.
53. Z. Kelemen, B. Péter-Szabó, E. Székely, O. Hollóczki, D. S. Firaha, B. Kirchner, J. Nagy and L. Nyulászi, *Chemistry – A European Journal*, 2014, **20**, 13002-13008.
54. L. Gu and Y. Zhang, *Journal of the American Chemical Society*, 2009, **132**, 914-915.
55. Z. Kelemen, O. Holloczki, J. Nagy and L. Nyulaszi, *Org Biomol Chem*, 2011, **9**, 5362-5364.
56. C. Shi, H. A. Hansen, A. C. Lausche and J. K. Norskov, *Physical Chemistry Chemical Physics*, 2014, **16**, 4720-4727.
57. J. H. Montoya, A. A. Peterson and J. K. Norskov, *Chemcatchem*, 2013, **5**, 737-742.
58. M. T. M. Koper, *Physical Chemistry Chemical Physics*, 2013, **15**, 1399-1407.